

# A Cryogenic Seven-Element HEMT Front End for DSS 13

J. Bowen and D. Neff

Radio Frequency and Microwave Subsystems Section

*A cryogenically cooled Ka-band (33.6-GHz), seven-element front-end array for the DSN has been built and tested. This system uses seven high-electron-mobility-transistor (HEMT) low-noise amplifiers cooled by a two-stage closed-cycle refrigerator. All system components from the polarizers to the output isolators are cooled to a physical temperature between 18 and 35 K. The noise temperatures of the individual elements range from 64 to 84 K over a 2.75-GHz bandwidth.*

## I. Introduction

There has been a desire to increase the operating frequency of the DSN for the purpose of improving telemetry capabilities to reduce spacecraft costs for a given performance. Although improvements in gain and bandwidth are achievable, problems associated with antenna deformations and focusing become significant. This currently limits the maximum operating frequency of the 70-m antennas to 8.4 GHz [1]. The use of an array of feeds has been suggested [2] and studied [3] as a method for correcting these problems. Digital signal combining techniques can then be utilized to recover the power losses associated with the antenna deformations [4].

This article describes an array front end built to demonstrate this technique at 32 GHz. The front end is described and its performance characteristics are documented.

## II. System Description

The input to the system consists of seven 22-dB-gain, smooth dual-mode feedhorns arranged in a triangular grid.

The feedhorns with associated mode generators, waveguide tapers, and vacuum windows bolt directly to the top plate of the vacuum jacket (Fig. 1 shows a block diagram of a single channel). Inside the jacket, a round-to-square waveguide transition is located between the feedhorn and the hybrid polarizer. The left circularly polarized (LCP) port of the polarizer is terminated while the right circularly polarized (RCP) port connects to a waveguide isolator that provides input isolation to the low-noise amplifier (LNA). At the output of the LNA is an output isolator similar to the isolator at the input. The output waveguide section is connected to the bottom plate of the vacuum vessel and serves as the connection to an external downconverter assembly, which contains follow-up filters and amplifiers.

These components were assembled in a single vacuum jacket, 35.5 cm in diameter and 91.4 cm long. Cryogenic cooling was provided by a single CTI model 1020 closed-cycle refrigerator (CCR) (CTI-Cryogenics, Waltham, MA). The amplifier bodies were cooled to less than 20 K by thermally connecting them to the CCR cold station with multiple layers of copper shim stock.

Thermal insulation at the input is provided by waveguide sections having a very high thermal resistance but low microwave loss (see Appendix A). The input round-to-square transition is a copper waveguide section suspended in a fiberglass tube. The room-temperature end of the transition is a brass flange bolted to the fiberglass tube. The cold end is a one-piece copper flange and waveguide that has no direct physical connection to the room-temperature flange of the top plate. The RF connection is achieved with a choked circular waveguide flange at the top. Additional heat straps are connected to the polarizers to bring their temperature down to 35 K. With the polarizers at 35 K and the amplifiers at 18 K, the remainder of the circuit components, waveguides, and isolators will all be within the range of 35 to 18 K.

At the output section, thermal insulation is provided by stainless-steel waveguide sections that have a thin copper plating on their interior surfaces. In each output channel are two sections, one that connects the room-temperature flange to the first stage of the refrigerator (70 K) and another that connects the first stage to the LNA output waveguide. A short piece of flexible waveguide is incorporated in each channel to relieve mechanical stress caused by thermal contraction.

A noise diode was provided for system calibration. The output of the noise diode was split by an eight-way power divider to each element of the array and coupled to each LNA by a 20-dB coupler. The noise diode has an excess-noise ratio (ENR) of 23 dB with 32 dB of coupling loss between the diode and each LNA input.

Figure 2 shows the completed front end with the vacuum vessel and radiation shield removed. Instrumentation is also shown.

### III. LNA Performance

The high-electron mobility transistor (HEMT) LNA's for the array were obtained from the National Radio Astronomy Observatory (NRAO), Charlottesville, Virginia [5]. These amplifiers are a four-stage single-ended design utilizing Fujitsu (FHR10X) HEMT transistors mounted in a gold-plated brass chassis with microstrip matching circuits on CuFlon. The LNA input and output waveguide transitions are E-plane probes coupled to a K-connector bead which then couples to the microstrip circuit. The LNA DC bias is supplied by a servo power supply externally located to the amplifier and vacuum vessel. This supply permits adjustment of the individual stage drain

voltage and regulated drain current but requires individual leads for drain and gate voltages to the amplifier.

At a physical temperature of 20 K, this LNA design provides a gain of 22 to 33 dB in the band of 26 to 36 GHz (26 to 29 dB at 32 GHz). The noise temperature varies between 33 and 63 K in the band of 26 to 36 GHz (52 to 59 K at 32 GHz). Figures 3 and 4 show the maximum, average, and minimum gain, respectively, and noise temperatures for the seven HEMT LNA's.

It should be noted that because of the large number of LNA's required for this project, there was no attempt to optimize the performance of each amplifier. Therefore, the large variation in performance is indicative of the kind of results to be expected in mass production.

## IV. System Performance

### A. Measurements

Noise-temperature and gain measurements were performed on the system prior to installation in a 34-m beam-waveguide antenna. The method of measurement consisted of hot and cold sources alternately placed over each feedhorn and measurement of the Y-factor (the ratio of the two output noise powers). The hot load consisted of a piece of microwave absorbing pad, the temperature of which was monitored with a mercury thermometer; the cold load was a section of the same type of absorbing pad immersed in liquid nitrogen. A waveguide filter with a passband of 31.20 to 33.95 GHz was placed at the output.

The receiver consisted of a follow-up amplifier, a precision adjustable attenuator, and a second follow-up amplifier. The output of the second follow-up amplifier was sent to the power meter directly without frequency conversion. The attenuator maintained the power level within the optimum range of the power-meter sensor.

The first follow-up amplifier was of the same NRAO design [5] as each of the array amplifiers. This provided a low-noise temperature (285 K at room temperature) and sufficiently broad bandwidth to cover the frequency band of the output filter.

Measurements were also performed to determine the gain of each channel and effective noise input provided to each channel by the noise diode. The gain was determined by placing an absorbing pad at room temperature at the feedhorn aperture and sampling the total output power (subtracting the power of the noise contribution by the

amplifier itself). Noise-diode temperature was determined by again placing an absorbing pad at the feedhorn aperture and sampling the power with the diode on and off. A  $Y$ -factor was determined and used, in turn, to calculate the noise temperature of the diode as seen at the LNA input.

## B. Results

Table 1 lists the values determined for effective input noise temperature as referenced at the feedhorn aperture,  $T_e$ , and the gain of each channel. The values for noise contribution by the front end,  $T_{fe}$ , were determined by subtracting the receiver temperature ( $T_{rcvr} = 285$  K) divided by the gain for that channel:

$$T_{fe} = T_e - \frac{T_{rcvr}}{\text{gain}}$$

The noise diode added 35.5 K  $\pm$  1.8 K at the front end.

## C. Error Analysis

The equation for noise temperature is

$$T_e = \frac{T_h - Y(T_c)}{Y - 1}$$

where  $T_e$  is the equivalent noise temperature of the front end as referenced at the feedhorn aperture,  $T_h$  is the physical temperature of the room-temperature pad, and  $T_c$  is the physical temperature of the liquid-nitrogen pad. The error in  $T_e$  can be characterized by [6]

$$\sigma T_e = \sqrt{\left| \frac{\partial T_e}{\partial T_h} dT_h \right|^2 + \left| \frac{\partial T_e}{\partial T_c} dT_c \right|^2 + \left| \frac{\partial T_e}{\partial Y} dY \right|^2}$$

or, in this case,

$$\sigma T_e = \sqrt{\left[ \left| \frac{1}{Y-1} \right| [\sigma T_h] \right]^2 + \left[ \left| \frac{Y}{Y-1} \right| [\sigma T_c] \right]^2 + \left[ \left| -\frac{T_c}{Y-1} - \frac{T_h - Y(T_c)}{(Y-1)^2} \right| [\sigma Y] \right]^2}$$

Here  $\sigma T_h$  is the error in the hot-load physical temperature,  $\sigma T_c$  is the error in the cold-load physical temperature, and  $\sigma Y$  is the error in the  $Y$  factor. The hot-load physical temperature is measured by a mercury thermometer inserted into the pad. The ability to accurately read the thermometer is limited to about 0.5 K, but the emissivity of the pad can vary by as much as 1 percent, which leads to an error at room temperature of as much as 3 K. At the liquid-nitrogen temperature, this 1-percent error will be much less significant, but the error in the temperature sensor will be on the order of 1 K.

Since the  $Y$ -factor is a ratio of the power measurements, its source of error rests in the errors of the power measurement. The  $Y$ -factor is calculated by

$$Y = 10^{\Delta P/10}$$

Here  $\Delta P$  is the difference between the power resulting from the hot load,  $P_h$ , and the power resulting from the cold load,  $P_c$ , in dB. The error in the  $Y$ -factor is

$$\sigma Y = \left[ \frac{\ln(10)}{10} \right] \left[ 10^{\Delta P/10} \right] (\sigma \Delta P)$$

where  $\sigma \Delta P$  is then the RMS error generated by the standard deviations in the individual power measurements [6]:

$$\sigma \Delta P = \sqrt{\sigma P_h^2 + \sigma P_c^2}$$

As a result, the error in the noise-temperature measurements is 3.0 K.

## V. Summary

A cryogenic seven-element Ka-band array front end has been assembled and tested. The system noise-temperature performance from 31 to 34 GHz varied from 64 to 84 K as referenced to the feedhorns.

This system can be applied to any antenna that suffers performance degradation due to surface deformations. Its relatively wide bandwidth should be attractive to radio astronomy applications as well as applications in deep-space telecommunications.

## Acknowledgments

The authors thank Marion Pospieszalski, Bill Lakatosh, and Ron Harris of National Radio Astronomy Observatory for development of LNA's and thermal isolators. Also, the authors thank Gary Bury, Juan Garnica, and Willard Smith for operational support at DSS 13, and Gary Glass for assistance with error analysis.

## References

- [1] P. W. Cramer, "Initial Studies of Array Feeds for the 70-Meter Antenna at 32 GHz," *TDA Progress Report 42-104*, vol. October–December 1990, Jet Propulsion Laboratory, Pasadena, California, pp. 50–67, February 15, 1991.
- [2] P. D. Potter, "64-Meter Antenna Operation at Ka-Band," *TDA Progress Report 42-57*, vol. March–April 1980, Jet Propulsion Laboratory, Pasadena, California, pp. 65–70, June 15, 1980.
- [3] S. J. Blank and W. A. Imbriale, "Array Feed Synthesis for Correction of Reflector Distortion and Vernier Beamsteering," *IEEE Trans. Antennas Propagation*, vol. AP-36, no. 10, pp. 1351–1358, October 1988.
- [4] V. A. Vilnrotter, E. R. Rodemich, S. J. Dolinar, Jr., "Real-Time Combining of Residual Carrier Array Signals Using ML Weight Estimates," *IEEE Trans. Communications*, pp. 604–615, March 1992.
- [5] M. W. Pospieszalski, J. D. Gallego and W. J. Lakatosh, "Broadband, Low-Noise, Cryogenically Coolable Amplifiers in 1 to 40 GHz Range," *1990 IEEE MTT-S International Microwave Symposium Digest*, pp. 1253–1256, 1990.
- [6] J. R. Taylor, *An Introduction to Error Analysis, The Study of Uncertainties in Physical Measurements*, Mill Valley, California: University Science Books, 1982.

## Appendix

### Waveguide Thermal Insulators for Vacuum Systems

#### I. Introduction

Waveguide thermal insulators are used in the various frequency bands to connect room-temperature signal waveguides to 15-K HEMT's or 4.2-K maser amplifiers. New devices have been constructed for use at X-, K-, and Ka-bands.

#### II. Description

A thermal insulator typically consists (see Fig. A-1) of a room-temperature flange, a shim providing an 0.08-mm gap, and a second cooled flange. The assembly is held and supported by an outer shell of G-10 fiberglass tube with a wall thickness of 0.76 mm. The gap dimension can be varied by simply changing the shim to the thickness desired; however, the 0.08-mm shim has proven optimum (at all frequencies) for the RF and thermal characteristics, providing a proper gap for room-temperature operation or when cooled below 15 K.

#### III. Performance

The performance at room temperature or cooled is typically less than  $-30$ -dB return loss and the insertion loss equivalent to a straight waveguide of the same length.

Having an abrupt change in the temperature gradient (hot to cold) simplifies the calculation of noise temperature for the various waveguide components as well as providing the maximum amount of cooled signal path.

The heat leak is difficult to measure; however, it appears to be no worse at 32 GHz than a stainless-steel waveguide of the same length with a thin copper-plated inside diameter (three skin depths).

#### IV. History

Transitions of this type have been constructed by a number of different organizations for different frequencies

and different applications. This adaptation was originally undertaken by Ron Harris and Sander Wienreb of National Radio Astronomy Observatory. Their design used a unit with a fixed gap; setting the gap dimension depended on the skill of the machinist. Setting the gap for use at the higher frequencies becomes much more difficult. The new JPL design makes it much easier to control the gap assembly at any frequency. An effect noticed after repeated cold cycling was the apparent growth of the G-10 fiberglass (from 2.54 to 5.08  $\mu\text{m}$ ). This was corrected by simply re-lapping the flange faces.

The fiberglass is held both with small screws for mechanical strength and an epoxy adhesive (Armstrong A-12) to reduce movement in the joint with repeated cooling cycles.

The latest unit developed for 32 GHz allows an 8.71-mm diameter round waveguide from an antenna horn to be connected—in only 50.8 mm of length—to a 5.64-mm square waveguide feeding a polarizer assembly (the device is constructed using the wire EDM technique). The polarizer output then goes to an HEMT amplifier at 15 K. A typical 4.5-K refrigerator system would require a second thermal isolator between 70 K and 4.2 K.

This design has been used in the 32-GHz reflected wave maser system, for the first 32-GHz R&D HEMT feed package at DSS 13 and the KABLE HEMT 33.6-GHz package recently delivered to DSS 13, in the WR-42 waveguide for the K-band (18- to 26-GHz) masers at the three 70-m sites, and for X-band HEMT testing in a 15-K CCR dewar.

#### V. Summary

A new component is now available for use with the higher frequency DSN CCR (vacuum) receiver systems; the component offers reliability, low thermal heat leak, and low microwave insertion loss.

**Table 1. Noise-temperature and gain values for each element.**

Element	Noise temperature with receiver, $T_e$ , K	Gain, dB	Front-end noise temperature $T_{fe}$ , K
1	71.4	25.3	70.6
2	64.2	26.6	63.6
3	77.0	25.3	76.2
4	65.7	26.3	65.0
5	85.2	24.6	84.2
6	80.9	27.1	80.3
7	68.9	28.1	68.5

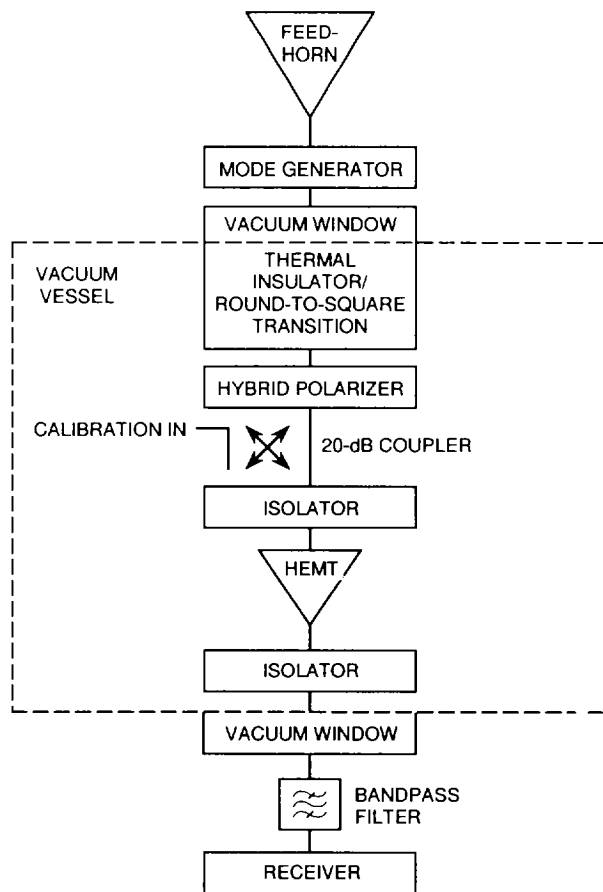
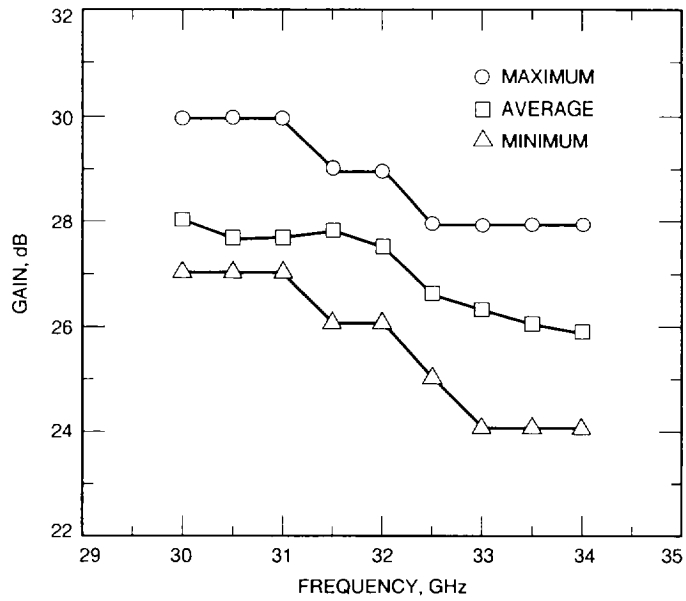


**Fig. 1. System block diagram of a single channel.**

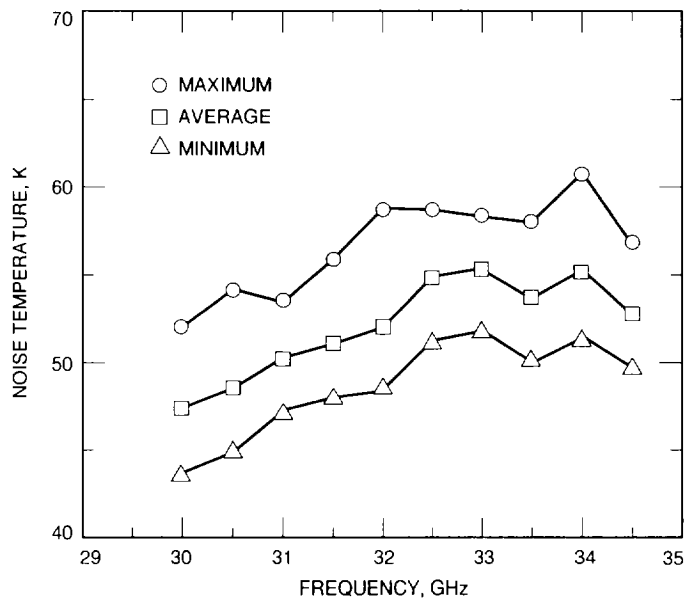


Fig. 2. The front end with vacuum vessel and instrumentation.





**Fig. 3.** The maximum, average, and minimum gain of the seven amplifiers as a function of frequency.



**Fig. 4.** The maximum, average, and minimum noise temperatures of the seven amplifiers as a function of frequency.

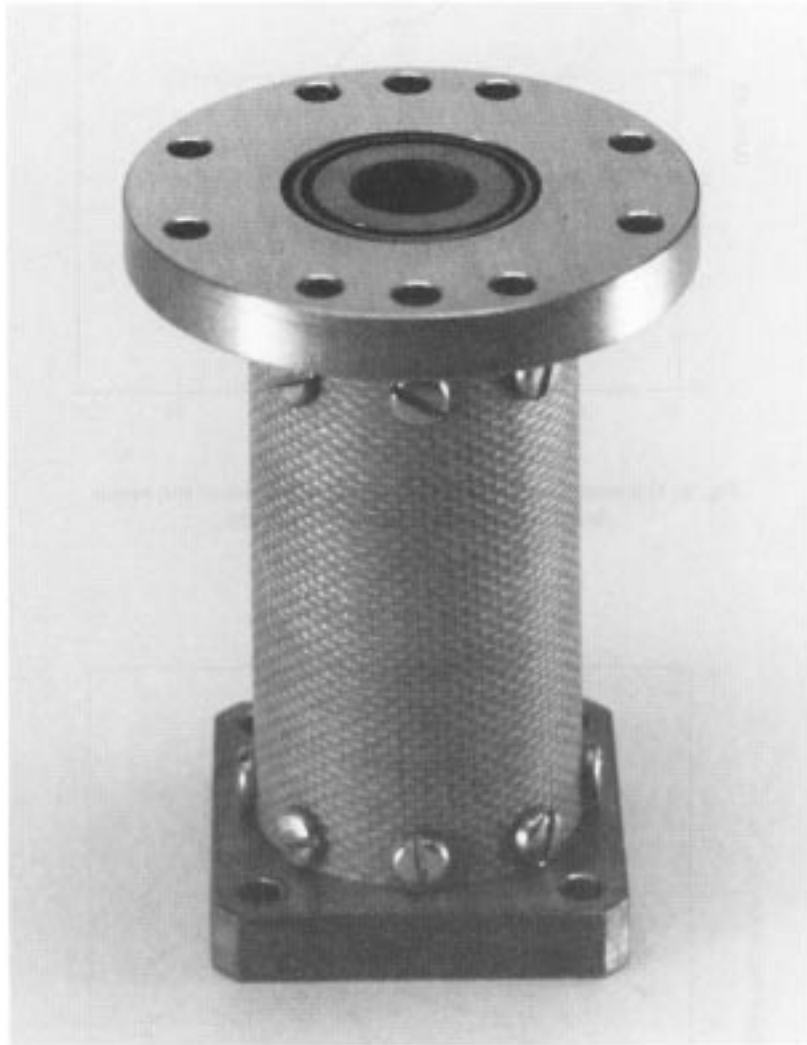


Fig. A-1. Thermal insulator for 32 GHz.